Analysis of New Aerodynamic Design of the Nose Cone Section Using CFD and SPH

Bogdan-Alexandru BELEGA*

*Corresponding author
Military Technical Academy, Department of Aircraft Integrated Systems and Mechanics, Blvd. George Coșbuc nr. 39-49, District 5, Bucharest, 050141, Romania
belega.bogdan@yahoo.com

DOI: 10.13111/2066-8201.2015.7.2.4

3rd International Workshop on Numerical Modelling in Aerospace Sciences, NMAS 2015,
06-07 May 2015, Bucharest, Romania, (held at INCAS, B-dul Iuliu Maniu 220, sector 6)
Section 2 – Flight dynamics simulation

Abstract: *A new nose cones concept that promises a gain in performance over existing conventional nose cones is discussed in this paper. It is shown that significant performance gains result from the adaptation of the exhaust flow to the ambient pressure. For this complex work, it was necessary to collect and study the various nose cone shapes and the equations describing them? The paper objective was to identify the types of nose cones with ejector channels and specific aerodynamic characteristics of different types of nose cones. The scope of this paper is to develop some prototype profiles with outstanding aerodynamic qualities and low cost for use in construction projects for missile increasing their range and effect on target. The motivation for such a work is caused by a lack of data on aerodynamics for profiles of some nose cones and especially improved aerodynamic qualities that can be used in designing missiles/ rockets. This design method consists of a geometry creation step in which a three-dimensional geometry is generated, a mathematical model presented and a simple flow analysis (FLUENT Simulation from SolidWorks2012 and ANSYS Simulation with SPH for fluid-structure interaction), step which predicts the air intake mass flow rate. Flow phenomena observed in numerical simulations during different nose cone operations are highlighted, critical design aspects and operation conditions are discussed, and performance characteristics of the selected nose cone are presented.*

Key Words: *nose cone, CFD, fluent, SPH, aerodynamic, fluid.*

1. INTRODUCTION

In my scientific work about nose cone with ejector channels, it was necessary to study the equations describing the various nose cone shapes.

This study also brought together some characteristics and nose cone information that I have tried to use to develop some prototype profiles with outstanding aerodynamic qualities and low cost for use in construction projects for missile increasing their range and effect on target. The objective of this paper is to show that boundary layer separation can be postponed by the shape of the rocket nose cone.

The idea here is to get the incompressible static pressure at the base of the forebody to be as large as possible.

This will give the greatest critical Mach number and the least adverse pressure gradient over the cylindrical afterbody. Although vortices cannot be avoided, they can be mitigated by using the best nose cone shape. Shapes that can produce high critical Mach numbers give

the greatest C_p with respect to ambient pressure. This is because the closer the C_p local minimum is to 0, the weaker the adverse pressure gradient becomes, which results in a small vortex strength. [3]

2. GEOMETRIC PROPERTIES OF NOSE CONES

The paper objective was to identify the types of nose cones and specific aerodynamic characteristics of different types of nose cones.

2.1 Geometry of Tangent Ogive

The Tangent Ogive is a body of revolution formed from a section of a circle as shown in Figure 1. Given the length to diameter ratio $\frac{L}{D}$, we need to determine two lengths to draw the half profile of an Ogive.

One length is the radius of the circle that describes the profile of the Ogive. The second length is the distance from the center of the defining circle to the center line of the Ogive. The equation for the tip of the Ogive is given by equation (1). The first equation in (1) is just the equation for a circle. This defines the profile of the Ogive from the base to the tip. The second equation defines the tip of the Ogive.

The *y* coordinate is equal to the length of the Ogive. The x coordinate (fig. 1) is related to the radius of the circle defining the Ogive and the diameter of the Ogive.

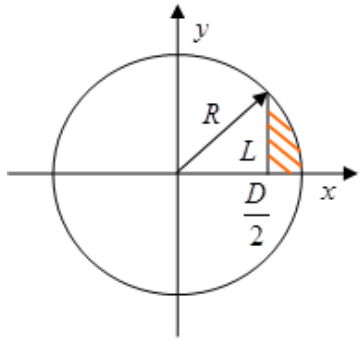

Fig. 1 - Tangent Ogive

$$\begin{aligned} x^2 + y^2 &= R^2 \\ x_L^2 + L^2 &= R^2 \end{aligned} \tag{1}$$

But $x_L = R - \frac{D}{2}$. So we have then

$$\begin{aligned} R^2 &= \left(R - \frac{D}{2}\right)^2 + L^2 \\ \left(R - \frac{D}{2}\right)^2 &= R^2 - L^2 \\ D &= 2 \cdot R - 2 \cdot \sqrt{R^2 - L^2} \end{aligned} \tag{2}$$

So now the $\frac{L}{D}$ is

$$\begin{aligned} &\frac{L}{D} = \frac{L}{2 \cdot \left(R - \sqrt{R^2 - L^2}\right)} = T \\ &L = 2 \cdot T \cdot \left(R - \sqrt{R^2 - L^2}\right) \\ &2 \cdot T \cdot \sqrt{R^2 - L^2} = 2 \cdot T \cdot R - L \end{aligned} \tag{3}$$

After simplifying, we get the following for the radius of the circle:

$$R = D\left(\frac{4 \cdot \left(\frac{L}{D}\right)^2 + 1}{4}\right) \tag{4}$$

For the distance from the center of the circle to the center line of the Ogive, we have

$$l = R - \frac{D}{2} = D \cdot \left(\frac{4 \cdot \left(\frac{L}{D}\right)^2 + 1}{4}\right) - \frac{D}{2} \tag{5}$$

After simplifying, we have for the distance to the center line:

$$l = D \cdot \left(\frac{4 \cdot \left(\frac{L}{D}\right)^2 - 1}{4}\right) \tag{6}$$

In order to simplify the next calculation, we need to create more compact notation by making the following assignments.

$$\begin{aligned} &T = \frac{L}{D};\ Y = \left(\frac{4 \cdot K^2 + 1}{4}\right); \\ &Z = \left(\frac{4 \cdot K^2 - 1}{4}\right) \\ &Y^2 - T^2 = Z^2;\ Y^2 + Z^2 = \frac{16 \cdot T^4 + 1}{8} \\ &Y \cdot Z = \frac{16 \cdot T^4 - 1}{16};\ Y + Z = 2 \cdot T^2;\ Y - Z = \frac{1}{2}; \\ &R = Y \cdot D;\ l = Z \cdot D \end{aligned} \tag{7}$$

2.2 Ogive wetted area

Another required ratio is that of the wetted surface area divided by the cross sectional area. The cross sectional area is simply

$$S_{ZU} = \frac{\pi \cdot D^2}{4} \tag{8}$$

The wetted surface is

$$S_w = \int_0^L 2 \cdot \pi \cdot r \cdot dy \tag{9}$$

where,

$$r = x - ZD = \sqrt{Y^2 \cdot D^2 - y^2} - ZD$$

Then the ratio is

$$\frac{S_w}{S_{ZU}} = \frac{2 \cdot \pi}{\pi \cdot \frac{D^2}{4}} \cdot \int_0^L r \cdot dy$$

$$= \frac{8}{D^2} \cdot \int_0^L \sqrt{Y^2 \cdot D^2 - y^2} \cdot dy - \frac{8}{D^2} \cdot \int_0^L Z \cdot D \cdot dy$$

$$= \frac{8}{D^2} \cdot \left[\frac{y \cdot \sqrt{Y^2 \cdot D^2 - y^2}}{2} + \frac{Y^2 \cdot D^2}{2} \cdot \sin^{-1}\left(\frac{y}{Y \cdot D} \right) \right]_0^L - 8 \cdot Z \cdot T \tag{10}$$

$$= 4 \cdot T \cdot \sqrt{Y^2 - T^2} + 4 \cdot Y^2 \cdot \sin^{-1}\left(\frac{T}{Y} \right) - 8 \cdot Z \cdot T$$

$$= 4 \cdot T \cdot Z + 4 \cdot Y^2 \cdot \sin^{-1}\left(\frac{T}{Y} \right) - 8 \cdot Z \cdot T$$

The ratio simplifies to

$$\frac{S_w}{S_{ZU}} = 4 \cdot Y^2 \cdot \sin^{-1}\left(\frac{T}{Y} \right) - 4 \cdot T \cdot Z \tag{11}$$

2.3 Ogive volume

The volume of the Tangent Ogive is:

$$V = \int_0^L \pi \cdot r^2 \cdot dy \tag{12}$$

where,

$$r = x - ZD = \sqrt{Y^2 \cdot D^2 - y^2} - ZD$$

The volume to area ratio is:

$$\frac{V}{D\cdot S_{ZU}}=\frac{\pi}{D\cdot\pi\cdot\frac{D^2}{4}}\cdot\int_0^L r^2\cdot dy=\frac{4}{D^3}\cdot\int_0^L\left(\sqrt{Y^2\cdot D^2-y^2}-Z\cdot D\right)^2\cdot dy=$$
$$=\frac{4}{D^3}\cdot\int_0^L\left(Y^2\cdot D^2-y^2\right)\cdot dy-\frac{4}{D^3}\cdot 2\cdot Z\cdot D\cdot\int_0^L\sqrt{Y^2\cdot D^2-y^2}\cdot dy+ \quad (13)$$
$$\frac{4}{D^3}\cdot\int_0^L Z^2\cdot D^2\cdot dy$$

$$\frac{V}{D\cdot S_{BT}}=\frac{4}{D^3}\cdot Y^2\cdot D^2\cdot L-\frac{4}{D^3}\cdot\frac{L^3}{3}-\frac{4}{D^3}\cdot 2\cdot D\cdot Z\cdot\left[\frac{y\cdot\sqrt{Y^2\cdot D^2-y^2}}{2}\right]_0^L-$$
$$-\frac{4}{D^3}\cdot 2\cdot D\cdot Z\cdot\left[\frac{Y^2\cdot D^2}{2}\cdot\sin^{-1}\left(\frac{y}{Y\cdot D}\right)\right]_0^L+\frac{4}{D^3}\cdot Z^2\cdot D^2\cdot L= \quad (14)$$
$$=4\cdot Y^2\cdot\frac{L}{D}-\frac{4}{3}\cdot\left(\frac{L}{D}\right)^3-Z\cdot\frac{8}{D^2}\cdot\left[\frac{y\cdot\sqrt{Y^2\cdot D^2-y^2}}{2}\right]_0^L-$$
$$-Z\cdot\frac{8}{D^2}\cdot\left[\frac{Y^2\cdot D^2}{2}\cdot\sin^{-1}\left(\frac{y}{Y\cdot D}\right)\right]_0^L+4\cdot Z^2\cdot\frac{L}{D}$$

$$\frac{V}{D\cdot S_{BT}}=4\cdot A^2\cdot K-\frac{4}{3}\cdot K^3-$$
$$-B\cdot\frac{8}{D^2}\cdot\left[\frac{y\cdot\sqrt{A^2\cdot D^2-y^2}}{2}+\frac{A^2\cdot D^2}{2}\cdot\sin^{-1}\left(\frac{y}{A\cdot D}\right)\right]_0^L+4\cdot B^2\cdot K$$

$$\frac{V}{D\cdot S_{BT}}=4\cdot A^2\cdot K-\frac{4}{3}\cdot K^3-B\cdot\frac{8}{D^2}\cdot\frac{L\cdot\sqrt{A^2\cdot D^2-L^2}}{2}-$$
$$-4\cdot B\cdot A^2\cdot\sin^{-1}\left(\frac{K}{A}\right)+4\cdot B^2\cdot K$$

$$\frac{V}{D\cdot S_{BT}}=4\cdot A^2\cdot K-\frac{4}{3}\cdot K^3-4\cdot B\cdot K\cdot\sqrt{A^2-K^2}- \quad (15)$$
$$-4\cdot B\cdot A^2\cdot\sin^{-1}\left(\frac{K}{A}\right)+4\cdot B^2\cdot K$$

$$\frac{V}{D\cdot S_{BT}}=4\cdot A^2\cdot K-\frac{4}{3}\cdot K^3-4\cdot B\cdot K\cdot B- \quad (16)$$
$$-4\cdot B\cdot A^2\cdot\sin^{-1}\left(\frac{K}{A}\right)+4\cdot B^2\cdot K$$

$$\frac{V}{D \cdot S_{BT}} = 4 \cdot A^2 \cdot K - \frac{4}{3} \cdot K^3 - 4 \cdot B \cdot A^2 \cdot \sin^{-1}\left(\frac{K}{A}\right) \tag{17}$$

3. DEVELOPPING OF A CONSTRUCTIVE SOLUTION FOR NOSE CONES WITH EJECTOR EFFECT. CASE STUDY.

To validate the numerical simulation performed in SolidWorks Flow Simulation Fluent, we used an existing model of an ogive of the 122mm caliber unguided rocket for which we already have experimental data.

The numerical simulations were performed first on the standard projectile of the 122mm caliber unguided rockets without modification of the nose cone part at different flight speeds up to its maximum speed– fig. 2.

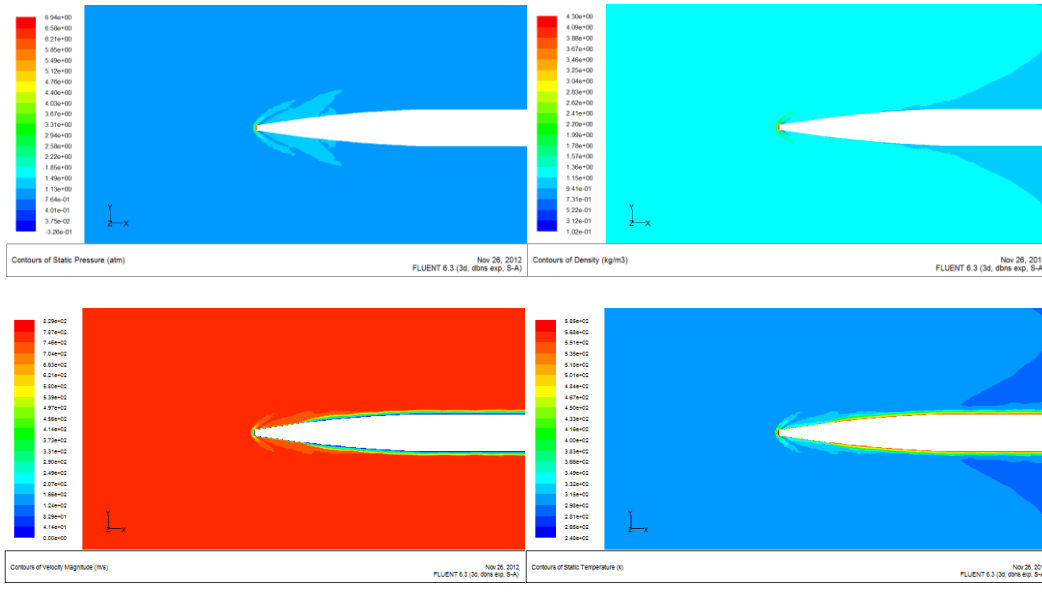

Fig. 2 – Pressure, velocity, density and temperature for simulation at 750 m/s

The results for simulations at different flight speeds are shown in Table 1.

Table 1 – Results of different velocities

Velocity (m/s)	Drag force for a quarter of structure (N)	Drag force to the rocket (N)
150	13.6	54.4
250	39.7	158.8
350	141.1	564.4
450	266.9	1067.6
550	366.8	1467.2
650	421.1	1684.4
750	493.1	1972.4

After selecting the channel configuration nose cone part ejectors (fig. 3 and fig. 4), we resumed the numerical simulations on the same type of projectile, this time equipped with modifications to the nose cone on the same flight speeds up to its maximum speed. In both cases, we extract the drag force produced at different levels of speed.

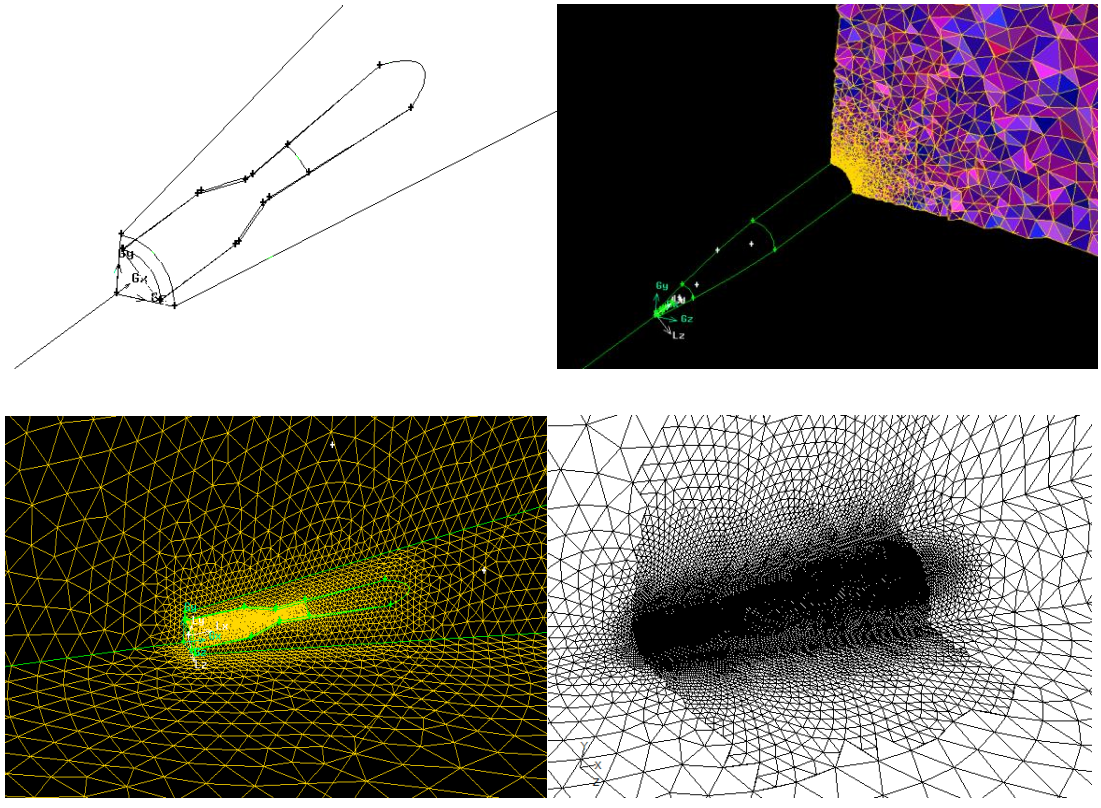

Fig. 3 – The selection of channels and mesh refinement in Gambit

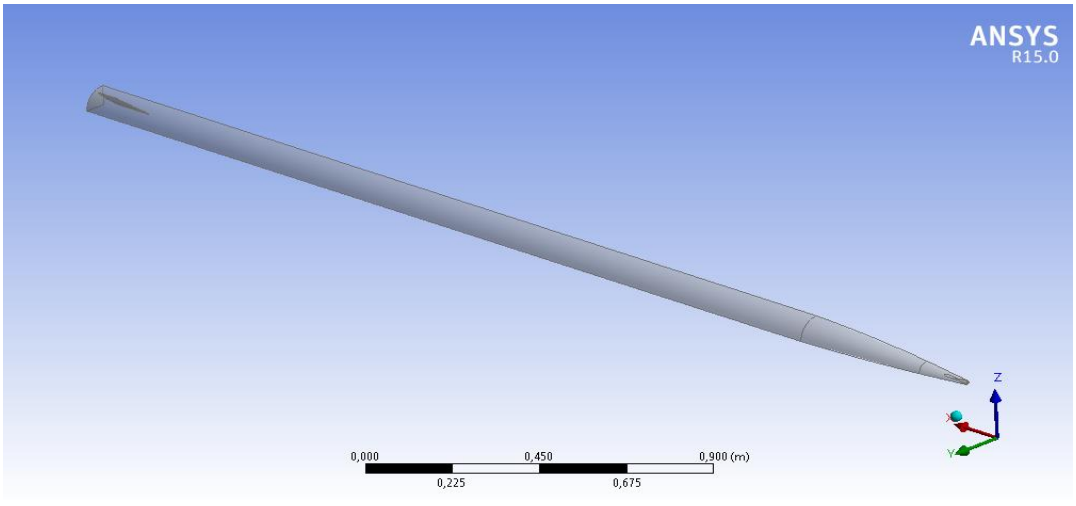

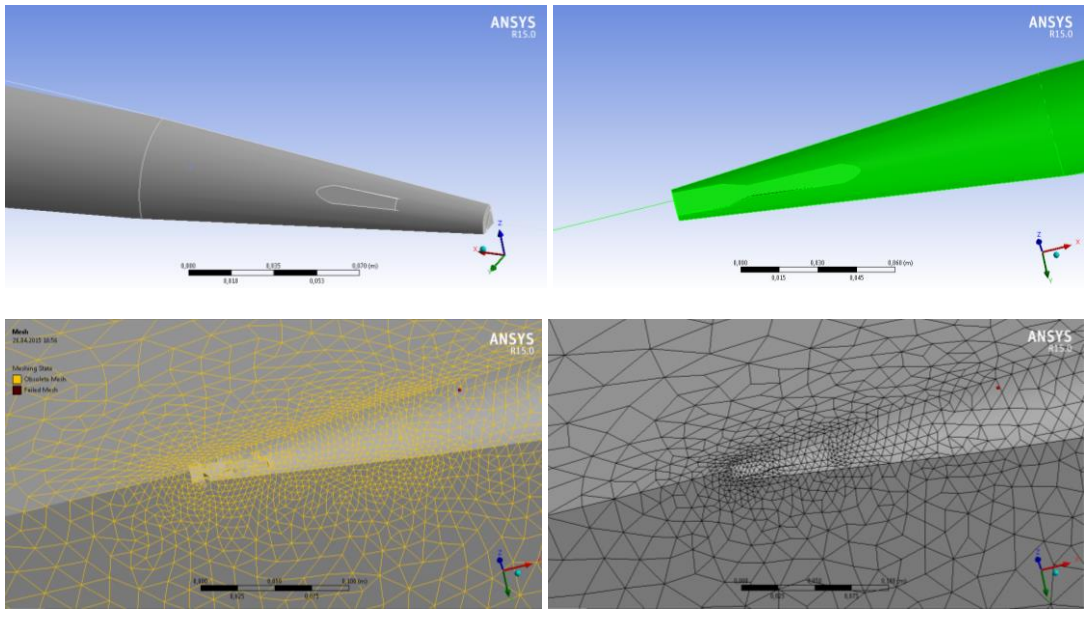

Fig. 4 – The selection of channels and mesh refinement in Ansys

The numerical simulations were performed first on the projectile standard 122mm unguided rockets caliber with modification of the nose cone part at different flight speeds up to its maximum speed.– fig. 5.

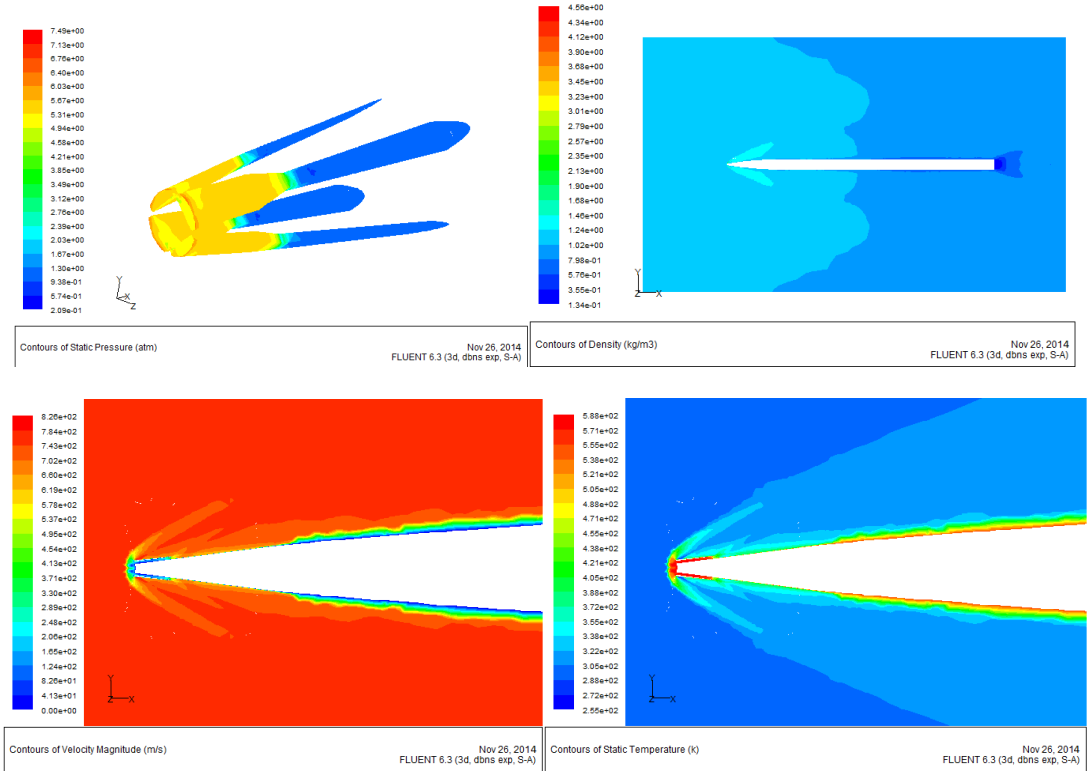

Fig. 5 – Numerical simulations to study the rocket nose cone equipped with ejector channels.

Numerical simulations have been performed to investigate the performance of the rocket nose cone equipped with ejector channels. The results for simulations at different flight speeds are shown in Table 2.

Table 2 – Results of different velocities

Velocity (m/s)	Drag force for a quarter of structure (N)	Drag force to the rocket (N)
150	13.3	53.2
250	37.1	148.4
350	122.2	488.8
450	254.4	1017.6
550	343.6	1374.4
650	385.5	1542.0
750	484.3	1937.2

4. CONCLUSIONS

The purpose of this paper is to propose a solution for performance improvement using missiles nose cone having ejector effect without disrupting the stability of the trajectory. The need was to achieve sustainable design solutions for ejector effect warheads for missiles in the execution of performance improvement over greater distances (fig. 6).

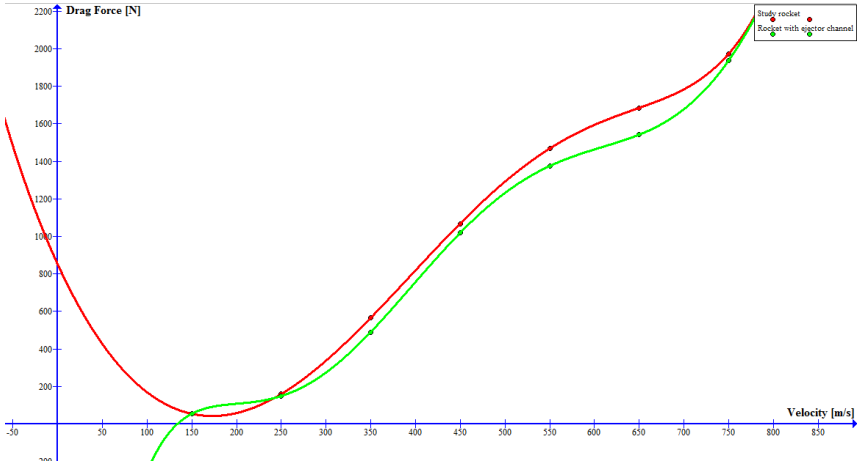

Fig. 6 – Chart compared to the amount of drag force for the two cases studied

The improvement in accuracy is achieved at considerably increased computational cost. The results showing the time evolution of the free surface of modified nose cone and the plots of the velocity field, show that the method is numerically efficient and stable.

Although comparable accuracy of numerical results can be achieved by employing other discrete methods, such as smooth particle hydrodynamics, finite volume or boundary element methods, owing to its significantly lower computational cost and the simplicity of numerical implementation, this method can be considered as a serious competitor for the older and better-established methods.

ACKNOWLEDGMENT

This paper has been financially supported within the project entitled "Horizon 2020 - Doctoral and Postdoctoral Studies: Promoting the National interest through Excellence, Competitiveness and Responsibility in the Field of Romanian Fundamental and Applied Scientific Research", contract number POSDRU/159/1.5/S/140106. This project is co-financed by European Social Fund through Sectorial Operational Programme for Human Resources Development 2007 - 2013. Investing in people!

REFERENCES

[1] C. Barbu, *Aerodinamica Computaţională*, Editura Academiei Tehnice Militare, Bucureşti, 2005.
[2] B.-A. Belega, *Balistica Exterioară şi Dinamica zborului rachetei – Balistica exterioară a proiectilelor activ-reactive*, ATM, Bucureşti, 2011.
[3] J. N. Nielsen, *Missile Aerodynamics*, Mc. Graw - Hill Book Company, Inc, New York, 1960.
[4] F. Moraru, B. Belega (Scobeniuc), A mathematical model for computing the trajectories of rockets in a resistant medium taking into account the earth's rotation (II). Mathematical model. *MTA Review*, vol. **XXI**, no. 3, 12 pag., Sept. 2010.
[5] G. A. Crowell Sr., *The descriptive geometry of the nosecone*, 1996.
[6] R. J. Felkel, Effect of Different Nose Profiles on Subsonic Pressure Coefficients, *American Institute of Aeronautics and Astronautics*, 2004.